Results in Nonlinear Analysis

ISSN 2636-7556

Peer Reviewed Scientific Journal

Numerical solution of a highly order linear and nonlinear equations using integrated radial basis function network method

Mayada G. Mohammed[1], Dmitry V. Strunin[2], Rajeev P. Bhanot[3]

[1]*Department of Mathematics, College of Education for Pure Sciences, University of Thi-Qar, Iraq;* [2]*School of Sciences, Faculty of Health, Engineering and Sciences University of Southern Queensland Toowoomba, Queensland 4350, Australia;* [3]*School of Chemical Engineering and Physical Sciences, Department of Mathematics, Lovely Professional University, Phagwara, Punjab 144411, India.*

In this work, we examine a variety of regimes of dynamicitygenerated using means of a single partial differential equation of sixth order nonlinearity), the NEP equationand equation (a single linear partial differential equation of sixth order) making use of the integrated radial basis function network method, a more sophisticated numerical technique (IRBFN). Previously, we used the Galerkin approach to generate NEP equation spinning solutions in one step. Firstly, we use the approach to replicate the previously found spinning regimes by solving the NEP equation. In the most recent round of numerical tests, we discover regimes that resemble whirling sequences of bends with one kink, two, or threeeach. Analysis is done on the changes in the distance between the kinks. Boundary conditions of two types are taken into consideration: periodic and homogenous. It is investigated how the dynamics rely on the domain's size and how bigger domains can support more spinning fronts. The kinks' direction of motion is determined by the initial state, but not their sizes or velocities. Secondly, We solve the Nikolaevskiy equation as an example for linear single partial differential equationusing IRBFN approach.
Key words and phrases: IRBFN, NEP
Mathematics Subject Classification (2010): 41A17, 11D04.

    Email addresses: mayadagassab20@utq.edu.iq (Mayada G. Mohammed); strunin@usq.edu.au (Dmitry V. Strunin); rajeevbhanot@yahoo.com (Rajeev P. Bhanot)

1. Introduction

Because of the vast range of nonlinear effects, the development of super-adiabatic structures in reaction fronts that are propagating, like spinning detonation and solid-phase combustion, piqued the curiosityof theorists and practitioners in mathematics. However, the first focus was on useful applications, such as the production of sophisticated materials through self-replicating at high temperatures (SHS). We refer to [1, 2, 3] for current experimental research in the field. A simple single-equation model that could replicate the spinning reaction fronts on a cylinder that were observed in experiments was created by Strunin in [4].

$$\frac{\partial u}{\partial t} = -\left(\frac{\partial u}{\partial t}\right)^2\left(\frac{\partial^2 u}{\partial^2 t}\right) + \left(\frac{\partial u}{\partial t}\right)^4 + \frac{\partial^2 u}{\partial^2 t} \tag{1.1}$$

It was also demonstrated later on [5] that Eq. (1.1) might characterize Certain non-local reaction-diffusion systems: nonlinear instabilities. For the sake of clarity, we shall refer to Eq. (1.1) as the equation for the nonlinearly energized phase (NEP)inrelation to those systems. The term "u" refers to the distance travelled by the combustion front (roughly a line dividing hot burned products from cold unburned mixture) along a hollow cylinder's axis in the context of the combustion fronts discussed in this study (Fig.1). Among the most remarkable experimentally observed regimes is the spinning front, which is one of the rich dynamics arising from the model (1.1). The solution in kink form (1.1) is shown in Fig. 1. In trials, the nearly vertical, steep portions in Figure 1.1 correspond to luminous hot areas. Spots with extremely high temperatures are frequently referred to as hyper adiabatic in combustion literature. Infiltration combustion experiments have also yielded similar hot-spot formations [3]. Lately, the compositions of combustion fronts in reactive compositions that vary have received particular attention. The impulsivedevelopment of regular structures, whose proportionalityis different from the original circumstances' symmetry, can occur alongside the combustion process regardless of the impact of early perturbations. In systems where the reaction products are blown through by the reactive gas towards the propagation front, it wasdemonstrated in 6 that the process of combustion could become unstable in systems where the explosive gasis blasted via the results of the reaction toward the spreadingahead, resulting in the creation of finger-shaped structures.
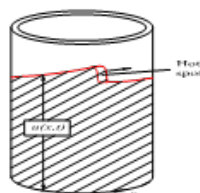
Fig. 1: Afront of reaction moving along a cylinder that is hollow.

Creation of structures resembling fingers. These mechanisms in order to spread a smolderingwave in a sawdust-filled channel shaped like a slit were experimentally investigated in [7]. Examining how scale parameters affect the instability that has occurred in the burningof very permeable media was the main goal. In [1, 2, 3], the structure of the metal powder combustion front exposed to the intrusion of natural gas was examined both experimentally and theoretically. The authors examined the dynamics of cellular wave structure initiation and propagation as well as the combustion of porous media through infiltration. They investigated how the quantity and form of cells were affected by the heterogeneous medium's controlling thermophysical parameters, the geometry pertaining to heat loss, the porous nature, etc.According to these findings, planar fronts can potentiallysplit into separate cells that travel through the layer of condensed material in a pulsating manner, leaving behind a belt of periodic-looking condensed combustion products in their wake.It is possible to replicate the qualitative nature of these regimes by applying Eq. (1.1). Based on principles of phenomenology, the

equation replicates the evolution of the front's shape while excluding concentration and temperature from its analysis. The fact that internal combustion enginesare frequently incredibly complicated and couldcontain a chain involving chemicalsprocesses involving multiple reactants that are compounded by a mechanical deformation, melting, etc., is evidence in favor of the phenomenological approach. Because of this, modeling the combustion systems with the use of the fundamental heat and concentration equations might become unfeasible. We can refer to [8, 9] which examined the granular gases' long-term cluster evolution, as an illustration of applying a phenological technique. Aldushin et al. in [10] made the initial effort to build a phenomenologically based model to describe the combustion waves rotating. Nonetheless, the front shape is more accurately described by the model (1.1). The shape is kink-like in [4], as seen in experimental observations, and sinusoidal in [10]. Furthermore, consistent with the experiments, the kink's motion decays completely if there is a significant enough heat loss into the external liquid. With respect to the formula, $v = \partial u/\partial x$, the curveresembles a soliton. More specifically, it's an auto-soliton, which is a kind of solitons found in living things. [11, 12]. This kind of solitons is distinguished from those in conservative systems by the prefix auto-. When energy release and dissipation are balanced, it results inthe auto-solitons, whereas how nonlinearity and dispersion are balanced produces the conservative solitons. A system with active-dissipative, in which energy is generated by chemical processes and dissipated by thermos conductivity, is commonly exemplified by the combustion front. The energy balance determines the distinct amplitude and velocity of an auto-soliton. The expression $(\partial u/\partial x)^2 \partial^2 u/\partial x^2$ denotes the energy release in Eq. (1.1), while the term $\partial^6 u/\partial x^6$ denotes the dissipation. The release and dissipation are linked by the phrase $(\partial u/\partial x)^4$ [5, 13, 16].

To make computations easier, we rewrite Eq. (1.1) as

$$\frac{\partial u}{\partial t} = -A\left(\frac{\partial u}{\partial t}\right)^2\left(\frac{\partial^2 u}{\partial^2 t}\right) + B\left(\frac{\partial u}{\partial t}\right)^4 + \frac{\partial^6 u}{\partial^6 t} \tag{1.2}$$

where B is conveniently assumed to be positive (the situation of B ispositive, changed to the situationof B negative by converting u to −u and B to −B). A and C are assumed to be positive. We can attain good accuracy and a somewhat short experiment time by varying the A, B, and C values. We do remark, however, that by rescaling u, x, and t, Eq. (I.2) can be changed to the canonical form (I.1). As a result, in rescaled coordinates, the outcomes of every experiment we do will also represent the answers to the classical Eq. (1.1). Equation (1.1) was previously resolved by applying the spectral Galerkinapproach [4], finite difference scheme, and 1D-IRBFN ethodology. In [14], a few first results were presented and talked upon. The more accurate IRBFN methodology, a collocation technique builton integrated radial basis function networks, is what we use in the current work [15, 16]. In section II, we apply the technique to acquire and examine a range of dynamics produced by the NEP formula (1.2), with various starting and boundary conditions. We also apply this method to solve Nikolaevskiyequation in section III. Conclusions are given in Section V.

II Numerical results for NEP equation

II. I. Regimes of Spinning Waves

For this section's experiments, we select the spatial domain's length to achieve spinning regimens. We select the spatial domain length that is compared to the bifurcation length, or, more specifically, the canonical the domain's lengthis greater compared to thebifurcation canonical extended. We stress such as the particularthe coefficients' valuesin the equation B, C, and Ahave no bearing on the form or motion of the front because each of the $u(x, t)$ graphs that are shown could be regarded jointly that corresponds to the standard version of Equation (I.2), albeit only using scaled coordinates.

A : One-Step Regime

Three numerical experiments are carried out in this paragraph using various initial conditions and periodic boundary conditions. A single-step spinning front is the resultant of the experiments.

1. First Experiment

The coefficients in the equation are: A = 7, B = 4, C = 3. Since $u(x, 0) = 3sinx$ is periodic, the initial condition is in line with the requirements for the boundaries. It appears that the dynamics persist because L is greater compared tothe bifurcation length. Following a period of transition (Fig. 2 right), the wave dynamic settles into the single-step structure depicted in (Fig. 2 left). Despite the initial condition's symmetry, the wave ultimately moves left rather than right. Since an optimally symmetric regime seems to be inherently unstable, It ultimately transforms entering either between the two conceivable regimes that are imbalanced (in this example, left-handed).
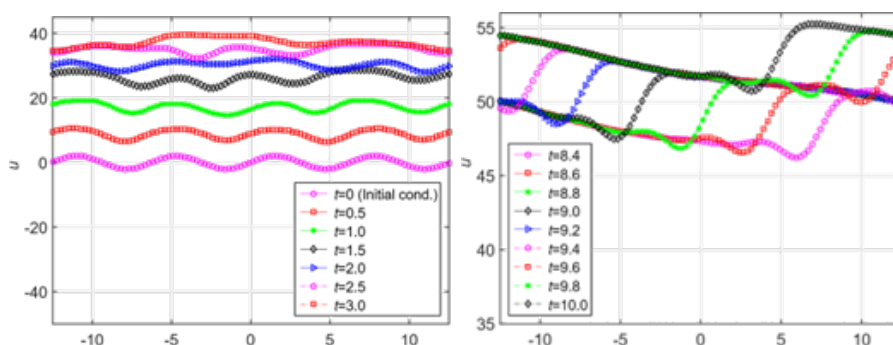
Fig. 2: First Experiment: (Right) The settled stage; (Left) The solution u versus x
at various times in the interim phase.

2. Second Experiment

The values A = 5, B = 4, and C = 3 are employed. The initial state is given by

$$u(x,0) = 1.3\ [sin(5x) + 1.5\ sin6x + x/6$$

Because the function's values on the right and left ends within the domain differ at $t = 0$, the initial condition in this experiment does not satisfy the boundary criteria. But as soon as the trial begins, the resolution $u(x, t)$ is compelled to meet the condition at the border, which results in that leftward huge move. As the original short-wavelength wave is rapidly smoothed down by the dissipation inconsistency (Fig. 3 left). After some time, the motion toward the right causes the one-step structure, or settled spinning regime, to establish (Fig. 3 right).
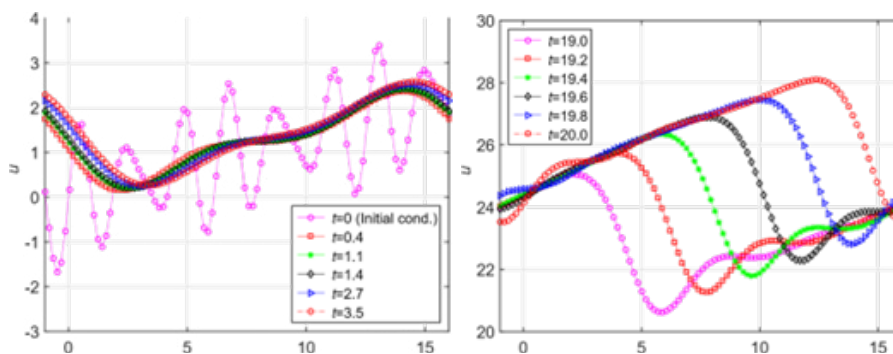
Fig. 3: Second Experiment: The relationship between the solution (u) and (x) at various points in the
stage of transition (left) and the established phase (right).

3. Third Experiment

We have selected A = 5, B = 2, and C = 3 as the equation coefficients. While Fig. 4 (right) depicts the resolution in the established state, Fig. 4 (left) depicts the dynamics at early stages. After some time, the front endures and advances to the right. With the x coordinate directed around the cylinder's perimeter, the regime observed here could be linked to the reaction front advancing in a rotating manner on a surface that is cylinder-shaped.

Once more, the initial condition in this experiment does not match the periodic boundary requirements. However, the big step on the left is caused by the instantaneous forcing of the solution $u(x, t)$ to fulfill boundary requirements. The intermediate step inside the computational domainthat is a component of the starting state has the opposite orientation (u increases in opposition to x) to this step (u decreases in opposition to x). The outcome is that the front is pushed to the right as a strong energy dischargebegins to take action in the vicinity of the sizable lately produced move. The new step is able in order to ascend above the first take a step in the centerand keep moving additionally to it since this action is strong enough. The spinning regime eventually settles rightward (Fig. 4 right).
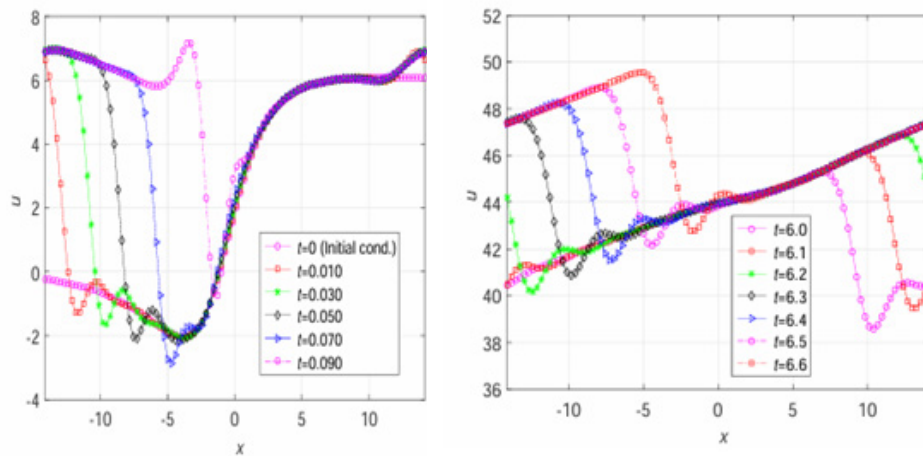
Fig. 4: Third Experiment the solution u versus x at various points in the transitional period (left) and the settled stage (right).

B. *A two-Step Regimes*

In this part, we carry out experiments with periodic and homogeneous boundary conditions using a larger computational domain.

1. *Fourth Experiment: Homogeneous boundary conditions*

The values of the coefficients in the equation are A = 3.5, B = 2.5, and C = 2. An elevated summit close to the left edge within the domain is selected as the first requirement. The peak can only travel to the right due to the left boundary's close closeness. When the initial peak's amplitude grows to a certain point, it becomes not one, but two kinks. The configuration is led by the lower kink, which is followed by the higher kink. The structure with two kinks settles as seen in Fig. 5 (left) after a brief period of transition (Fig. 5 right).
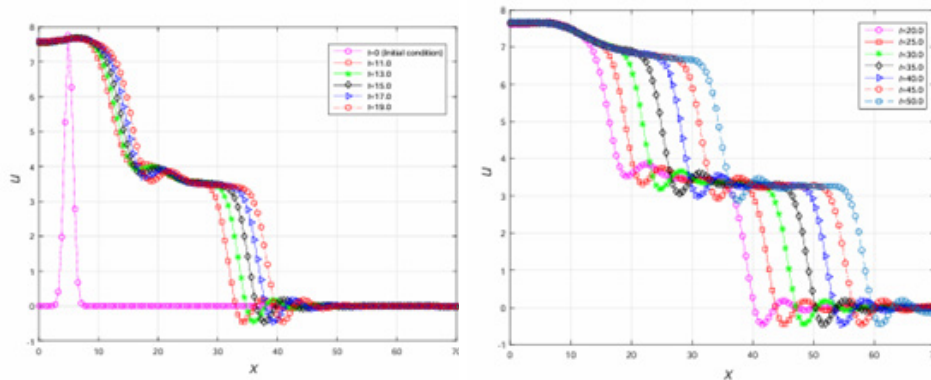
Fig. 5: Fourth Experiment: The solution u versus x at various points in the transitional period (left); Settled stage (right).

Fifth Experiment: Boundaries that are periodic

A = 7, B = 2, and C = 1 are the selected equation coefficients. The initial state exhibits many oscillations each period in a sinusoidal shape.

The one-step regime's spatial domain is smaller than this one. Trial 1. Around $t = 21$, the structures develop after a period of transitional dynamics (Fig. 6 left). A helical path is shown by a linked configuration of two kinks that travel from upper right to left when the cylinder-shaped figure plane is rolled (Fig. 6 right).
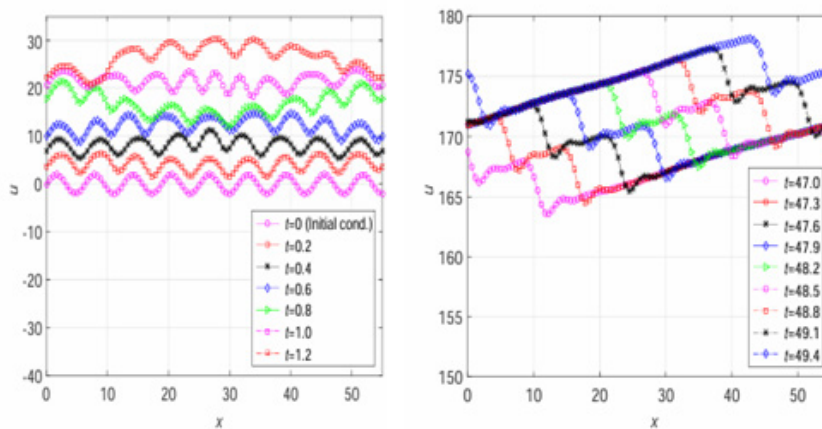
Fig. 6: The solution u versus x at various points in the stage of transition(left) as well as the established state (right).

C. A Three-PhaseRegimes

Sixth Experiment: Boundaries that are homogenous

The domain size and the original condition's amplitudein Experiment 6 are greater than all of thoseof the earlier experiments. The coefficients in the formulas are A = 3, B = 2, and C is equal to 2. The beginning amplitude is increased from 7.8 to 8.2 in comparison to the fourth Experiment. This aids in creating the third phase, as seen in Figs. 7 (left), along with the larger do main available. Fig. 7 (right)

shows the progressive appearance of the three-step structure following a time of transition Fig. 7 (left). The third step is still in the stage of formation, but the first two completely developed leading steps with separate horizontal plateaus are served. Observe that the first step's highest point is directly on top of the tiny sub-peak before the following phase.
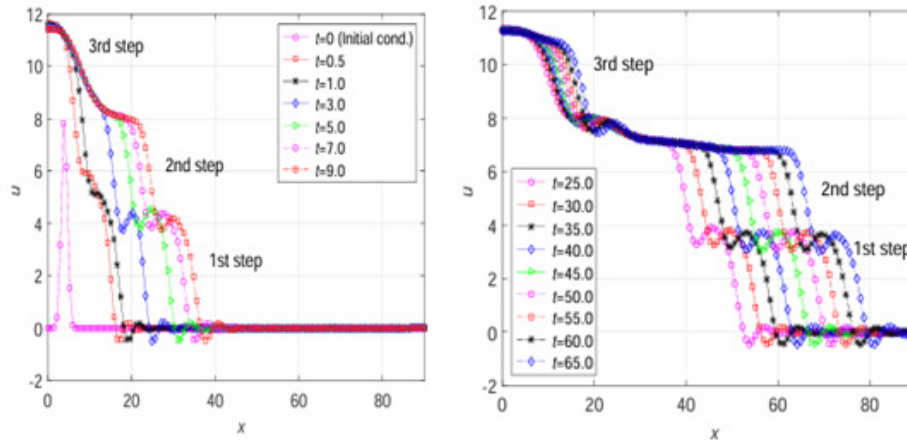
Fig. 7: The solution (right) settled stage; (left) the relationship between u and x at various points in the transitional period.

III Numerical solution for Nikolaevskiy equation

The Nikolaevskiy equation was first presented as a model for seismic waves. It can also be used to simulate a wide range of systems, such as electro convection and reaction-diffusion systems, that contain a neutral "Goldstone" mode. At least when the dispersive elements in the equation are suppressed, it is known to display chaotic dynamics at the beginning of pattern generation. Comparing with NEP equation, Nikolaevskiy equation has linear excitation in relation to reaction diffusion systems while NEP equation has nonlinear one.

$$\frac{\partial u}{\partial t} = a\left(\frac{\partial^2 u}{\partial^2 x}\right) + b\left(\frac{\partial^4 u}{\partial^4 x}\right) + c\left(\frac{\partial u}{\partial t}\right)^2 + d\frac{\partial^6 u}{\partial^6 x'}$$

linear excitation denoted by the term of fourth order $b\left(\frac{\partial^4 u}{\partial^4 x}\right)$, where b > 0. The expansion is restrained by the nonlinear component $c\left(\frac{\partial u}{\partial t}\right)^2$, which transfers the energy to higher modes where a damping force of 6 u is predominant.

Seventh experiment with homogenous conditions

We solve Nikolaevskiy equation as $a = 1$, $b = 1$, and C = 1 and $d = 1$ are the selected equation coefficients. The starting pointis $u(x, 0) = 5*Exp - (x–2)^2$. Fig. 8 (left) shows the initial state and Fig. 8 (right) represent the steady state.
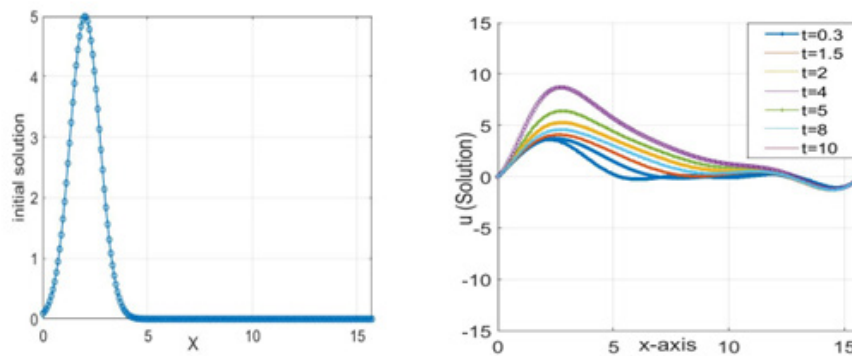
Fig. 8: The initial state(left) and the steady state(right).

Conclusion

We combined the IRBFN approach using the Picard iteration method in one step to solve NEPandNikolaeviskii equations. For NEP equation, the spinning regimes that were previously achieved in [4] using the Galerkin numerical approach were successfully recreated by the method. In this work, a much greater range of the dynamics are examined. Different initial conditions and two distinct kind of boundary conditions: periodic and homogenous—were employed. Regimes with only one stage areproduced by the first three experiments; two-step regimens areproduced by experiments 4 and 5; and Experiment 6 yields three-phaseregimes. For Nikolaevskiy equation, we run one experiment using homogenous conditions.

Acknowledgement

References

[1]   S. V. Kostin, P. M. Krishenik, N. I. Ozerkovskaya, A. N. Firsov, K. G. Shkadinskii, Cellular filtration combustion of porous layers, Combust. *Ex plos. Shock Waves* 48 (2012) 1–9 (2012). https://doi.org/10.1134/S0010508212010017

[2]   S. V. Kostin, P. M. Krishenik, K. G. Shkadinskii, Experimental study of the hetrogeneous filtration combustion mode, Combust. *Explos. Shock Waves* 50 (2014) 42–50 (2014). https://doi.org/10.1134/ S0010508214010055

[3]   S. V. Kostin, P. M. Krishenik, K. G. Shkadinskii, Pulsating cellu lar regimes of infiltration combustion of porous media, *Russ. J. Phys. Chem*. B 9 (2015) 385–391 (2015). https://doi.org/10.1134/ S1990793115030069

[4]   D. Strunin, Autosoliton model of the spinning fronts of reaction, *IMA J. Appl. Math.* 63 (2) (1999) 163–177 (1999). https://doi.org/10.1093/imamat/63.2.163

[5]   D. Strunin, Phase equation with nonlinear excitation for nonlocally coupled oscillators, *Phys. D Nonlinear Phenom*. 238 (18) (2009) 1909–1916 (2009). https://doi.org/10.1016/j.physd.2009.06.022

[6]   A. Aldushin, T. Ivleva, Hydrodynamic instability of the coflow filtration combustion: numerical simulation, *Dokl. Phys. Chem*. 451 (2013) 157–160 (2013). https://doi.org/10.1134/S0012501613070038

[7]   A. Aldushin, B. S. Braverman, Saffman-taylor problem in filtration com bustion, *Russ. J. Phys. Chem*. B 4 (2010) 788–792 (2010). https://doi.org/10.1134/S1990793110050143

[8]   S. Das, S. Puri, Pattern formation in the inhomogeneous cooling state of granular fluids, *Europhys. Lett.* 61 (2003) 749–755 (2003). https://doi.org/10.1209/ epl/i2003-00292-4

[9]   I. Aranson, L. Tsimring, Pattern and collective behavior in granular media: Theoretical concepts, *Rev. Mod. Phys.* 78 (2006) 641–692 (2006). https://doi.org/10.1103/RevModPhys.78.641

[10]   A. P. Aldushin, B. A. Malomed, Zel'dovich, Phenomenological theory of spin combustion, *Combust. Flame* 42 (1981) 1–6 (1981). https://doi.org/10.1016/0010-2180(81)90137-1

[11]   M. C. Cross, P. C. Hohenberg, Pattern formation outside of equilibrium, *Rev. Mod. Phys* 65 (1993) 851–1111 (1993). https://doi.org/10.1103/RevModPhys.65.851

[12]   B. Kerner, V. Osipov, Autosolitons, *Physics-Uspekhi* 32 (2) (1989) 101–138 (1989).

[13] D. Strunin, M. Mohammed, Range of validity and intermittent dynamics of the phase of oscillators with nonlinear self-excitation, *Commun. Nonlinear Sci. Numer. Simul.* 29 (1–3) (2015) 128–147 (2015). https://doi.org/10.1016/j.cnsns.2015.04.024

[14] A. Bretas, D. Wen. Security of Wireless Communications against Eaves-dropping and Attacks by Using Shannon's Theory. *International Journal of communication and computer Technologies* 12.1 (2024) 76–85.

[15] N. Mai-Duy, T. Tran-Cong, Numerical solution of differential equations us ingmultiquadric radial basis function networks, *Neural Netw.* 14 (2) (2001) 185–199 (2001). https://doi.org/10.1016/S0893-6080(00) 00095-2

[16] D. Ngo-Cong, F. Mohammed, D. Strunin, A. Skvortsov, N. Mai-Duy, T. Tran-Cong, Higher-order approximation of contaminant transport equation for turbulent channel flows based on centre manifolds and its numerical solution, *J. Hydrol.* 525 (2015) 87–101 (2015). https://doi.org/10.1016/j.jhydrol.2015.03.038

[17] H. P. Langtangen, S. Linge, Finite Difference Computing with PDEs - A Modern Software Approach. *Springer Nature*, Cham, 2010 (2010).

[18] M. Mortensen, H. P. Langtangen, G.N. Wells, Afenics-based programming framework for modeling turbulent flow by the reynolds-averaged navier stokes equations, *Adv. Water Resour.* 34 (9) (2011) 1082–1101 (2011). https://doi.org/10.1016/j.advwatres.2011.02.013

[19] B. Arunalatha, C. Paidimarr, Development of Low Power GNSS correlator in Zynq SoC for GPS and GLONSS. *Journal of VLSI circuits and systems*. 6.2 (2024) 14–22.